SIMULATION OF NEAR FIELD DILUTION OF THE SUBMARINE OUTFALL OF SANTA MARTA (COLOMBIA)

SIMULACION DE LA DILUCION DE CAMPO CERCANO DEL EMISARIO SUBMARINO DE SANTA MARTA (COLOMBIA)

FRANCISCO GARCÍA
M.Sc. Professor, Universidad del Magdalena, fgarcia@unimagdalena.edu.co

CARLOS PALACIO
Ph.D. Professor, Universidad de Antioquia, cpalacio@udea.edu.co

GUSTAVO CHANG
M.Sc. Professor Universidad del Magdalena, gchang@unimagdalena.edu.co

ABSTRACT: The dilution, trajectory and thickness of the buoyant plume formed by wastewater discharge from the submarine outfall of Santa Marta were determined using a near field dilution model and hydrographic data from salinity, temperature and density profiles, as well as from the velocity data at different levels of the water column. The magnitude of the velocity was provided by previous runs of a three-dimensional hydrodynamic model. The results showed that the plume goes through alternating periods of entrapment in the water column or reaching the water surface, according to conditions of upwelling and stratification of the receiving body of water. When the plume comes to the surface, dilution levels greater than 100 are achieved.

KEY WORDS: submarine outfall, dilution, stratification, near field dilution.

RESUMEN: Se determinaron la dilución, trayectoria y espesor de la pluma boyante generada por la descarga de aguas residuales del emisario submarino de Santa Marta, usando un modelo de dilución para campo cercano y datos hidrográficos de perfiles de salinidad, temperatura y densidad, al igual que datos de velocidad a diferentes niveles de la columna de agua. La magnitud de la velocidad fue suministrada mediante corridas de un modelo hidrodinámico en tres dimensiones. Los resultados mostraron que la pluma presenta períodos alternados de afloramiento a la superficie o atrapamiento en la columna del agua, según las condiciones de surgencia y estratificación del cuerpo receptor de agua. Cuando la pluma aflora a la superficie, se lograr niveles de dilución superiores a 100.

PALABRAS CLAVE: Emisario submarino, estratificación, dilución de campo cercano

1. INTRODUCTIÓN

The management of wastewater generated in domestic and industrial activities is performed by various treatment methods, reuse and disposal. The selection of a management scheme is determined by specific economic and technological considerations such as cost, the availability and complexity of technology, and the implications of possible effects on the environment.

The ocean has a huge natural assimilating capacity to minimize the adverse effects of the discharged wastewater, a feature that is taken advantage of by many coastal communities to dispose of wastewater using submarine outfall systems [1]. The implementation of these systems is based on reduced operating costs, low technological complexity and minor effects on the environment [2, 3]. The discharged wastewater systems with diffusers produce a rapid dilution of the effluent, decreasing concentrations of toxic substances and other materials to very low levels [4-6]. This phenomenon of rapid mixing of wastewater and sea water is known as initial dilution or near field dilution [7]. The initial dilution depends primarily on discharges of wastewater, diffuser length, the depth of discharge, ambient currents and density stratification [8]. After ejection from the outfall diffusers, the sewage effluent plumes rise rapidly through the water column due to their buoyancy relative to the surrounding ocean waters. As they rise, they are diluted by entrainment of the ambient ocean water resulting in a gradual increase in plume density. If the receiving ambient has a uniform density profile along the water column, the mixture of wastewater/sea water reaches to the water

surface. However, in a density stratified sea environment, the mixture usually rises to a level of equilibrium in which the density of the mixture is equal to the density of the sea water [1, 9].

Mixing processes usually take place in two zones, where different physical mechanisms dominate. The first process occurs as a result of the buoyancy and momentum of the discharge. This zone is called the "near field". The "far field" is when initial turbulence decays and mixing takes places as a result of turbulence generated by ocean currents [5]. In this paper the near field of the Santa Marta outfall is shown.

Near field models are used to predict where the plume will eventually reach a trap level, the thickness of the plume, and the dilution achieved at the limit of this near field zone [4, 5]. The behavior of plumes in the near field has been studied using various models such as CORMIX [10] RSB [11] UPLUME, UOUTPLM, UDKHDEN, UMERGE and ULINE [12]. The early works that were used to develop models of this type considered only density differences between the discharge and the receiving environment, without taking physical characteristics into account. Later research by Rouse, et al. [13], Priestley and Ball [14], and Morton [15], included the physical characteristics of the discharge. Fan [16] examined the trajectory, thickness and dilution of buoyant plumes in both stratified and unstratified environments. These were among the first models that included the wastewater plume elevation (submergence depth of plume from surface). Based on Fan [16] research, models for determining dilution in the near field have evolved to consider output from multiple diffusers. Models of the latest generation also include initial conditions of buoyancy and momentum, consider entrainment of the plume in the receiving environment, and take into account density and velocity values from different levels of the water column in the calculation. This article presents the results of application of the PLUME3 model developed and validated by Tate [17] in order to determine the trajectory, thickness and dilution of the effluent plume caused by the submarine outfall in the bay of Santa Marta.

2. MATERIALS AND METHODS

2.1. Study Area

The Coastal Area of Santa Marta (CASM) has a latitude between 11.21° and 11.31° N and 74.18° and 74.24° W in the Caribbean Sea (Figure 1), The climate regime is

characterized by a dry season (December-April), in which the "Alices" (north east winds) produce the local phenomenon of upwelling, reducing the water temperature (20°-25°C), and increasing wave intensity and salinity (up to 38 UPS). In the rainy season (May-November) upwelling stops; the water is warmer (27°-29°C) and the salinity drops to 34 UPS [18].

2.2. Dilution Model

The Lagrangian plume dilution model formulated by Tate [17] was used, which considers an element of volume Δt and surface area DA that rises within a receptor fluid (Figure 2). The element is moved along a path L with a velocity $u_i=(u,v,w)$ through the fluid, which in turn moves with velocity $U_i=(U_x, U_y, U_z)$. The coordinate system shown in Figure 2 indicates that the horizontal plane is formed by the X and Y axes, while the Z plane indicates the vertical direction. The governing equations are given in differential form in equations (1) to (5). Five equations are shown for conservation of mass, momentum in X, Y, and Z, and buoyancy as an expression of energy conservation.
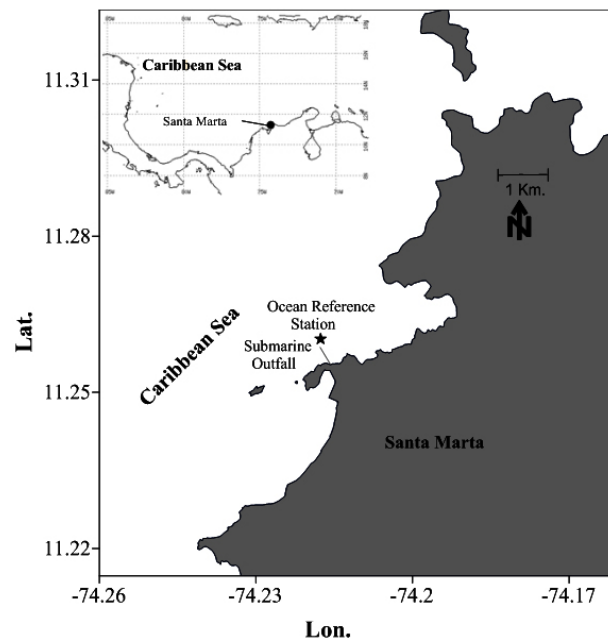

Figure 1. Location of the CASM and the Ocean Reference Station

These equations are given six variables: u, v and w are the velocity magnitude of the plume in x, y, and z directions as mentioned previously. A is the surface area, V is the volume, and g' is the buoyancy modified by gravity. In the latter, the density of discharge and of the receiving flow (ρ, ρ_a), respectively, are involved, as well

as the, the horizontal components (U_x, U_y) and the vertical component (U_z) of the ambient velocity and the change of the system buoyancy N^2.

Mass conservation: $\dfrac{\partial(\rho V)}{\partial t} = \rho_a \alpha U_{ent} A$,   (1)

x-momentum: $\dfrac{\partial(\rho V u)}{\partial t} = U_x \dfrac{\partial(\rho V)}{\partial t}$,   (2)

y-momentum: $\dfrac{\partial(\rho V v)}{\partial t} = U_y \dfrac{\partial(\rho V)}{\partial t}$,   (3)

z-momentum: $\dfrac{\partial(\rho V w)}{\partial t} = U_z \dfrac{\partial(\rho V)}{\partial t} + \rho g' V$,   (4)

Buoyancy: $\dfrac{\partial(g' V)}{\partial t} = -N^2 w V$; $N^2 = \dfrac{g}{\rho}\dfrac{\partial \rho_a}{\partial z}$,   (5)

The source code of the PLUME3 model developed by Tate [17] was rewritten in Matlab 7.0 (MathWorks) in order to be coupled to the 3D hydrodynamic model. It was run with velocity, temperature and salinity data, in several layers of the water column to discover the dilution, trajectory, and the submergence level of discharged wastewater.
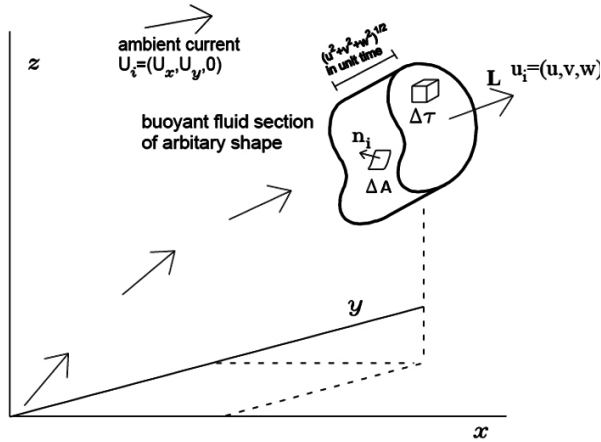
Figure 2. Schematics discharge fluid moving in the receiving body of water (Tate [17]).

The model was previously validated for various conditions by Tate [17], and has been used in similar studies as reported by Miller [9]. Among the marine conditions considered by Tate [17], there were some similar to those found in the Santa Marta bay [19]: unstratified (December-April and Julio) and stratified ambient fluid (April-June; August-Novenber). For this reason the model was considered appropriate.

2.3. Hydrodynamic Model

The model "RMA10" was used [20] in order to simulate the

state variables, pressure, and velocity in three dimensions, by solving a group of equations based on: Navier-Stokes' equations, mass conservation equation, advection-diffusion equation, and state equation (in order to relate density, salinity, temperature, and suspended sediments). Bottom roughness, Coriolis effect, and roughness induced by the wind on the free surface, are also included in the model [21]. This model estimates levels of free surface and horizontal components of velocity in tridimensional fields of flow. Hydrodynamic equations are solved by the finite element method, using Galerkin's method of weighed residuals. Spatial integration is carried out using the Gauss quadrature method, by customizing the unsteady variables in time using the Crank-Nicholson modified method [21, 22]. The solution is totally implicit and the group of simultaneous equations is solved by the Newton-Raphson nonlinear iteration. The governing equations are given in differential form in Cartesian coordinates in equations (6) to (11).

Movement equations:

$$\rho.\left(\frac{\partial u}{\partial t} + u\frac{\partial u}{\partial x} + v\frac{\partial u}{\partial y} + w\frac{\partial u}{\partial z}\right) - \frac{\partial}{\partial x}\left(\varepsilon_{xx}\frac{\partial u}{\partial x}\right) -$$
$$\frac{\partial}{\partial y}\left(\varepsilon_{xy}\frac{\partial u}{\partial y}\right) - \frac{\partial}{\partial z}\left(\varepsilon_{xz}\frac{\partial u}{\partial z}\right) + \frac{\partial p}{\partial x} - \Gamma_x = 0,$$ (6)

$$\rho.\left(\frac{\partial v}{\partial t} + u\frac{\partial v}{\partial x} + v\frac{\partial v}{\partial y} + w\frac{\partial v}{\partial z}\right) - \frac{\partial}{\partial x}\left(\varepsilon_{yx}\frac{\partial v}{\partial x}\right) -$$
$$\frac{\partial}{\partial y}\left(\varepsilon_{yy}\frac{\partial v}{\partial y}\right) - \frac{\partial}{\partial z}\left(\varepsilon_{yz}\frac{\partial v}{\partial z}\right) + \frac{\partial p}{\partial y} - \Gamma_y = 0,$$ (7)

$$\rho.\left(\frac{\partial w}{\partial t} + u\frac{\partial w}{\partial x} + v\frac{\partial w}{\partial y} + w\frac{\partial w}{\partial z}\right) - \frac{\partial}{\partial x}\left(\varepsilon_{zx}\frac{\partial w}{\partial x}\right) -$$
$$\frac{\partial}{\partial y}\left(\varepsilon_{zy}\frac{\partial w}{\partial y}\right) - \frac{\partial}{\partial z}\left(\varepsilon_{zz}\frac{\partial w}{\partial z}\right) + \frac{\partial p}{\partial z} + \rho.g - \Gamma_z = 0 ,$$ (8)

Continuity equation:

$$\frac{\partial u}{\partial x} + \frac{\partial v}{\partial y} + \frac{\partial w}{\partial z} = 0,$$ (9)

Advection-diffusion equation:

$$\frac{\partial s}{\partial t} + u\frac{\partial s}{\partial x} + v\frac{\partial s}{\partial y} + w\frac{\partial s}{\partial z} - \frac{\partial}{\partial x}\left(D_x\frac{\partial s}{\partial x}\right) - \frac{\partial}{\partial y}\left(D_Y\frac{\partial s}{\partial y}\right)$$
$$- \frac{\partial}{\partial z}\left(D_z\frac{\partial s}{\partial z}\right) - \theta s = 0,$$

(10)

Equation of state:

$$\rho = F(s),$$ (11)

Where x, y, z = Cartesian coordinates; u, v, w = velocities in the directions of the Cartesian system; t = time; P = pressure of water, D_X, D_Y, D_Z = Eddy diffusion coefficients; ε_{xx}, ε_{xy}, ε_{xz}, ε_{yx}, ε_{yy}, ε_{yz}, ε_{zx}, ε_{zy}, ε_{zz} = Eddy turbulence coefficients; g = acceleration of gravity, r = density of water; Γx, Γy, Γz = external forces; S = salinity; and θs = source / sink of salinity.

2.4. Sampling

Data from the Ocean Reference Station (ORS) was used as input to the direct plume dilution model. It was located 0.5 km offshore of Santa Marta at 11.23° N, 74.22° W, where the diffusers of the submarine outfall are located (Figure 1). The hydrographic data were obtained using a Water Level Recorder (WLR) 7 (Aanderaa) equipped with sensors for pressure (0 - 700kPa), temperature (Thermistor: Fenwall GB32JM19 from -3 to 35 ° C) and conductivity (Conductivity Cell 3094 0-77 mmho/cm). Two measurements per month were taken from January to December 2009. At the ORS, equipment was slowly lowered into the water column to measure pressure, temperature and conductivity. This information was then used to derive the salinity and density, calculated by means of the equation of state for seawater [23, 24]. Characterization of the discharged wastewater was done using the composite sampling flow-proportional technique [25] in the pumping station, that forces water to the seabed. To determine the depth of the thermocline, the threshold method was used. This method seeks a level in the water column at which the temperature profile (or density profile) changes at a predefined value relative to reference points at the surface [26].

3. RESULTS AND ANALYSIS

3.1. Profiles of temperature, salinity and density

The thermohaline conditions and density are shown in Figures 3 and 4. The shadow regions in the figures show the range of the parameter according to the measurements. The data between January and March revealed a well-mixed surface layer where vertical profiles of temperature, salinity and density are almost uniform. Strongest upwelling occurs in this period [27] due to the intense Caribbean low-level jet of NE trade winds [28]. There are two seasons during in which clear periods of stratification occur; from late April to June, and from August to December. During these periods

the difference between surface and bottom temperature on the ocean is clear. Temperatures range from 26 to 30 ° C and densities are less than 35, practical salinity units (PSU) have been measured [19].

The temporal variation of the temperatures in the water column during the CASM study were measured, with a minimum value of 22.3 °C and a maximum of 30.2 °C, for the months of January and August, respectively. The average for the year (2009) was 26.2 °C. From December to April surface temperatures were below the annual average, while from May to November they exceeded this value, except for July, when a considerable drop in temperature occurred due to the lower upwelling period. The details of the thermohaline conditions at Santa Marta Bay are referred to in Garcia et al., [19].

Extreme values of 35.6 and 36.5 PSU were measured for salinity in August and April, respectively, indicating an annual variation of 0.9 PSU. The average for the year was 36.1 PSU. The salinities above the annual average were recorded between January and July and those below the average were from August to December. As for surface density, extreme values of 22 and 24.8 kg/m3 were recorded in the months of August and January. The annual average was 24 kg/m3. Densities were high from January to April and low from May to December. The level of stratification begins from a depth of 3 meters in the water column, with thicknesses of up to 13 meters and maximum gradients of 0.679 ° C/m. The details of the calculation in order to determine the thickness of the thermocline and the thermal gradients in the water column during the CASM study are referred to in Garcia et al., [19].

3.2. Characteristics of the discharge

The composition and quantity of wastewater discharged by the submarine outfall are presented in Table 1, according to the measurements of this study. Besides the average flow used in the simulations to determine the dilution, the table shows the Biochemical Oxygen Demand (BOD) and the Chemical Oxygen Demand (COD), total solids, suspended and dissolved solids, nitrogen, phosphorus, fats and oils. The characterization of the discharge revealed a typical composition for domestic wastewater with a BOD / COD of around 30%, and a high content level of solids.
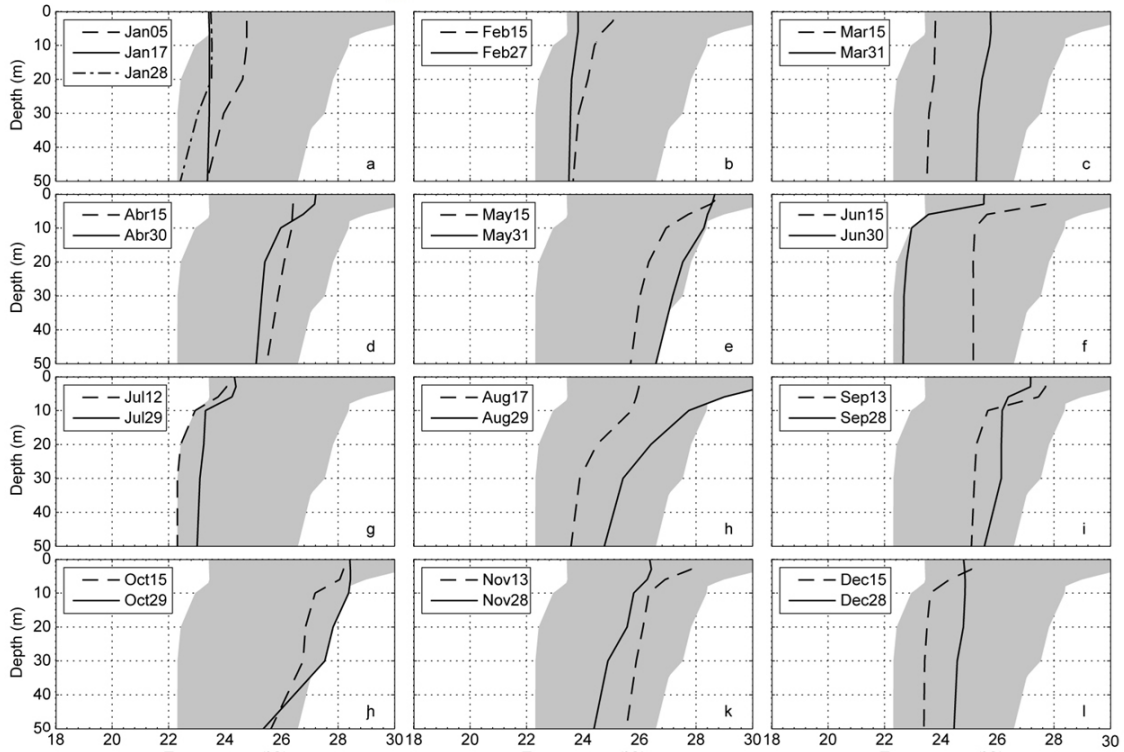
Figure 3. Temperature profiles, with two temperature profiles per month. a) Jan; b) Feb., c) Mar., d) Apr., e) May., f) Jun., g) Jul., h) Aug., i) Sep., j) Oct., k) Nov., l) Dec.
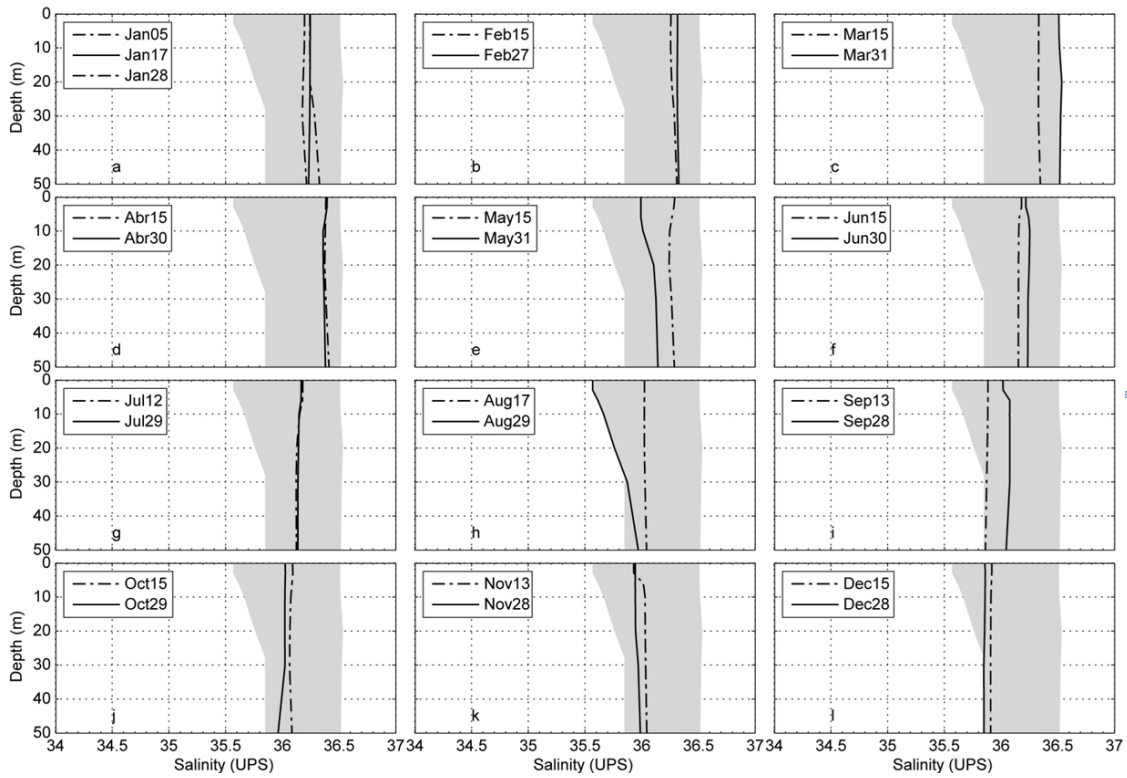
Figure 4. Salinity profiles. Two salinity profiles by months. a) Jan; b) Feb., c) Mar., d) Apr., e) May., f) Jun., g) Jul., h) Aug., i) Sep., j) Oct., k) Nov., l) Dec.

3.3. Hydrodynamic Conditions

The hydrodynamic conditions in CASM were obtained with RM10 model. The velocity values $U_i=(U_x, U_y, U_z)$ simulated with the RM10 model were using in the dilution model. Details of the calibration and validation process of the RM10 model at CASM are referred to in Garcia et al., [20,29].

3.4. Entrapment levels of the plume

PLUME3 model graphical outputs of plume centerline elevation (solid line) and plume boundaries (dotted lines) for a single diffuser are presented in figure 7. The diffuser is located at the end of the diffuser section of the outfall pipe. The results for other diffusers are similar. From December to April and July, the wastewater plume reaches the sea surface. This phenomenon coincides with periods of upwelling, when temperature, salinity and density profiles are uniform in the water column. This behavior happens twice a year; corresponding to upwelling of greater duration and intensity from December to March, and a shorter upwelling period between June and August. The wastewater plume was submerged between April and June and from September to December; simulations of the submergence depths of the plume from the surface gave results between 25 and 45 m.

Table 1. Characteristics of the plume from the submarine outfall of Santa Marta

	Flow (L/s)	DQO (mg O₂/L)	DBO₅ (mg O₂/L)	Total Solids (mg/L)	Dissolved Solids (mg/L)	Suspended Solids (mg/L)	Total Nitrogen (mg/L)	Total Phosphorous (mg/L)	Fats and Oils (mg/L)
Maximum	1784	896	698	2780	1198	2004	49	22	22
Minimum	715	411	199	598	400	104	21	8	6
Standard Deviation	163.9	97.2	547.7	216.4	412.8	339.5	7.2	4.4	4.5
Average	1028.64	650.84	289.24	1029	650.76	378.24	32.88	15.4	13.04
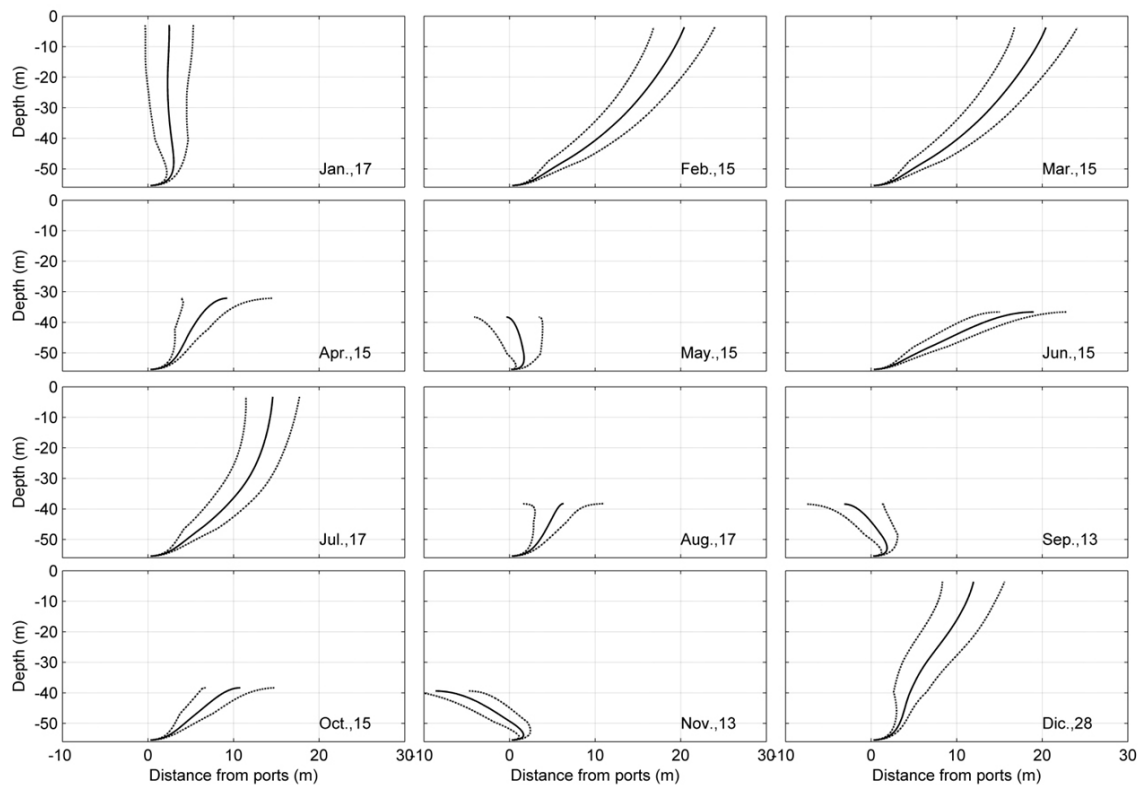
Figure 7. Wastewater discharge plume centerline elevation (solid line) and plume boundaries (dotted lines)

Figure 8 shows the calculated dilution from biweekly data of temperature, density, salinity and velocity profiles of the water column. Dilutions (dashed line) are highest in January, when upwelling phenomenon occurs. Depth

of submergence (solid line) is also shown in Figure 8. When the plume reaches the surface of the water column, dilutions are greater than 100:1, which happens from December to March and in July. During periods of stratification, the plumes were trapped at different levels. When the plume gets trapped, the dilution is low, reaching values up to 10:1; in this scenario the plume does not reach the sea surface. In the near field, effluents rise in the water column, and at the same time the ambient seawater is entrained into the plume, resulting in a rapid dilution of the effluent. In a density stratified sea environment, the mixture usually rises to a level of equilibrium in which the density of the mixture is equal to the density of the sea water. At this level the plume attains neutral buoyancy and the entrainment of ambient water stop.

4. DISCUSSION AND CONCLUSION

Submerged discharges by multiple diffusers are an effective way to dispose of degradable liquid waste in bodies of water. We examined the last diffuser of the Santa Marta submarine outfall in order to depict the behaviors of the disposal system. In this study it was found that all diffusers, including the first one, that is closer to the shore, have the same behavior as the last one. Taking one diffuser as typical, in order to represent the behavior of all the diffusers in the system, is a common practice in near field simulation. In

this study measurements of salinity and temperature profiles were combined with simulations of velocity in the water column, to determine the dilution and plume height of the wastewater disposal in Santa Marta bay. Impacts on the environment can be controlled and limited to small areas since a high degree of dilution can be achieved by employing these systems. The level of dilution achieved depends on hydrographic conditions and stratification, the depth of the water column, ocean currents and characteristics of the effluent diffuser. The PLUME3 model was used in this study because it can predict the plume trajectory, dilution, and the depth of entrapment. Although the dilution in the near field of submarine outfalls has been the subject of mathematical models and many laboratory studies, there are few field studies, due to the difficulty and cost of mapping, and the changing conditions of the environment, especially when the plume is trapped by stratification [30]. Comparison between simulations and field measurements also requires the determination of many parameters that make the task complex [30]. There are few plume models having a documented and complete formulation, including a full test in laboratory conditions and that have been documented for various field scenarios that permit their validation. The PLUME3 model has these characteristics and is available for free. The source code is accessible and permits coupling with hydrodynamics models. The PLUME3 model was selected with this criterion in mind.
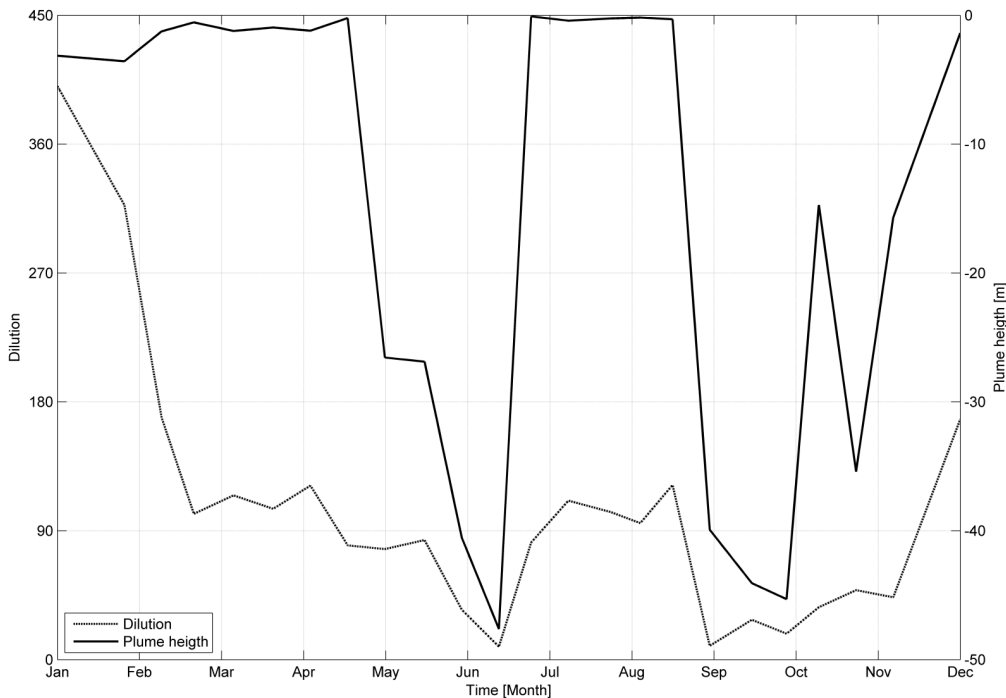
Figure 8. Plume rise height (solid line) and dilution (dashed line) of the Santa Marta submarine outfall

Submarine outfall plumes rise up to surface or are entrapped depending on environmental conditions in the receiving body due to the density change of the water column. The plume rises up to surface when the temperature and density profiles are uniform throughout the water column, coinciding with local upwelling periods reported for this area of the Caribbean Sea. It was shown that during the two periods of upwelling that occurs between December and April and July, when the buoyant plume of the outfall reaches the surface, dilutions greater than 100, sometimes up to 400 are reached. When the plume comes to the surface of the water, its thickness varies between 5 and 20 meters. In this scenario, the plume reaches the surface in a diluted form. When the plume reaches the level of neutral buoyancy by entrapment due to stratification of the water column, dilution has the maximum value of 10:1. In these cases, the plume remains trapped at depths between 47 and 25 meters without affecting the surface of the water. Determining the plume entrapment level is extremely important for quantification of the effect of solar radiation in the rate of bacterial decay. In the scenario where the plume reaches the surface, it arrives diluted, and solar radiation contributes to increased reduction of bacteria. In periods of entrapment, solar radiation is not relevant to bacterial decay since levels of neutral buoyancy are lower than those of photic depth. In these cases, the salinity contributes to decrease of bacteria [31]

ACKNOWLEDGEMENTS

REFERENCIAS

[1] Muhammetoglu, A., Yalcin, O.B. and Ozcan, T., Prediction of wastewater dilution and indicator bacteria concentrations for marine outfall systems, Marine Environmental Research, 78, pp. 53-63, 2012.

[2] Metcalf. and Eddy. Wastewater Engineering, Treatment, Disposal and Reuse. USA: McGraw-Hill. 1991

[3] Yang, L., Review of marine outfall systems in Taiwan, Water Science and Technology, 31, pp. 257–264, 1995.

[4] Kim, Y., Kang, S., Seo, W. and Oh, B., Far-field Transport of Effluent Plumes Discharged from Masan Sea Outfalls, Ocean Research, 22(2), pp. 69-80, 2000.

[5] Tian, X., Roberts, P. and Daviero, G., Marine Wastewater Discharges from Multiport Diffusers. I: Unstratified Stationary Water, Journal of Hydraulic Engineering, 130(12), pp. 1137–1146, 2004.

[6] Blumberg, F., JI, Z. and Ziegler, C., Modeling outfall plume behavior using far field circulation model, Journal of hydraulic engineering, 122, pp. 610-616, 1996.

[7] Kang, S.W., Oh, B., Park, K.S. and You, S., Near-field Dilution of Wastewater Effluents Discharged from Submerged Ocean Outfalls in Masan Bay, KSCE Journal of Civil Engineering, 3(4), pp. 395- 405,1999.

[8] Fischer, H.B., List, E.J., Koh, R.C.Y., Imberger, J. and Brooks, N.H., Mixing in inland and coastal waters. Academic Press, New York, 1979.

[9] Miller, B., Peirson, W.L., Wang, .Y. C. and Cox, R. J., An Overview of Numerical Modelling of the Sydney Deepwater Outfall Plumes, Marine Pollution Bulletin, 33(7-12), pp. 147-159, 1996

[10] Jirka, G.H. and Akar, P.J., Hydrodynamic classification of submerged multiport-diffuser discharges. J. Hydr. Engrg. 117(9), pp. 1113-1128, 1991.

[11] Roberts, P.J. and Snyder, W., Hydraulic model study for Boston outfall II, Environmental Performance. J. Hydr. Engrg. 119(9), pp. 988-1002, 1993.

[12] Muellenhoff, W. P., Soldate, A., Baumgartner, D., Schuldt, M. D., Davis, L. and Frick, W., Initial mixing characteristics of municipal ocean discharges. U.S. Environmental Protection Agency. Washington. D.C: 1985.

[13] Rouse, H., Yih, C.S. and Humphreys, M. W. Gravitational convection from a boundary source, Tellus, 4, 201-210, 1952: en: Initial Mixing characteristics of municipal ocean discharges: Volume I. Procedures and applications. United States Environmental Protection Agency. pp. 201-210, 1985.

[14] Priestly, C.H. and Ball, F.K. Continuous convection from an isolated source of heat. Quarterly J. of the Royal Meteor. Soc. 81, 1955. En: Initial Mixing characteristics of municipal ocean discharges: Volume I. Procedures and applications. United States Environmental Protection Agency. pp. 144- 157, 1985

[15] Morton, B.R., Forced plumes, J. of fluid Mech.5,1959. En: Initial Mixing characteristics of municipal ocean discharges: Volume I. Procedures and applications. United States Environmental Protection Agency. 151-163, 1985

[16] Fan, L.H. and Brooks, N.M., Turbulent mixing phenomena of ocean outfalls. J. San. Eng. Div., Am. Soc. Civ. Eng. 92, 1959. En: Initial Mixing characteristics of municipal ocean discharges: Volume I. Procedures and applications. United States Environmental Protection Agency. pp. 296-300, 1985.

[17] Tate, P.M., The rise dilution of buoyant jets and their behavior in an internal wave field. [PhD Thesis]. School of Mathematics Faculty of Science University of New South Wales. Sydney. P. 109, 2002.

[18] Vega, J., Rodriguez, A., Reyes, M.C. y Navas, R., Formaciones coralinas del área de Santa Marta: estado y patrones de distribución espacial de la comunidad bentónica, Bol. Invest. Mar. Cost., 37, pp. 87-105, 2008.

[19] Garcia, F.F., Palacio, C. y Garcia, U., Distribución vertical de temperatura y salinidad en el área costera de Santa Marta (Colombia), Dyna, 171, pp. 232-238, 2012.

[20] Garcia, F.F., Palacio, C. and Garcia, U., Simulation of hydrodynamic condictions at Santa Marta coastal area (Colombia), Dyna, 174, pp. 119-126, 2012.

[21] Fossati, M. and Piedra, I., Numerical modeling of residual flow and salinity in the Rio de la Plata, Applied Mathematical Modeling. 32, pp. 1066–1086, 2008.

[22] Palacio, C., Garcia, F.F. y García, U., Calibración de un modelo hidrodinámico 2D para la bahía de Cartagena, Dyna, 164, pp. 152166, 2010.

[23] Fofonoff, P. and Millard, R., Algorithms for computation of fundamental properties of seawater, Unesco technical papers in marine science. París, France, 1983.

[24] UNESCO. Processing of oceanographic station data. Unesco technical papers in marine science. París, France, 1991.

[25] Kim, N.T. and Bengtsson, B.E., Design of a representative and cost-effective sampling programs for industrial wastewater with examples from bleached kraft pulp and paper mills, Resources, Conservation and Recycling,18, pp. 107 124, 1996.

[26] Holte, J. and Talley, L., A new algorithm for finding mixed layer depths with applications to Argo data and subantarctic mode water formation, J. Atmos. Oceanic Technol., 26(9), pp. 1920-1939, 2009.

[27] Reichel, G. y Jimeno, M., Caribe Colombia. Available: http://www.banrepcultural.org/blaavirtual/geografia/carcol/biblio1.htm [citado 8 de Enero de 2011]. [citado 18 de Diciembre de 2012].

[28] Eidens, C., Bayraktarov, E., Pizarro, V., Wilke. T. and Wild. C., Seasonal upwelling stimulates primary production of Colombian Caribbean coralreefs. Proceedings of the 12th InternationalCoral Reef Symposium, Cairns, Australia, 9-13 July 2012. Available: http://www.icrs2012.com/proceedings/manuscripts/ICRS2012_6C_1.pdf

[29] Garcia, F.F., Chang, G. and Palacio. C., Calibración y validación de un modelo 3D para el área costera de Santa Marta (Colombia), Rev. Fac. Ing. Univ. Antioquia, 62, pp. 177-188, 2012.

[30] Hunt, C., Mansfield, A.D., Mickelson, M., Albro, C., Rockwell, W. and Roberts, P.J.W., Plume tracking and dilution of effluent from the Boston sewage outfall. Marine Environmental Research, 70, pp. 150-161, 2010

[31] Deluque, M., Garcia, F.F. and Palacio, C., Determinación del T90 en la bahía de Santa Marta (Col.), Dyna 167, pp. 122-131, 2011.